

**Multi-wavelength Study of Magnetic Field and Turbulence in the Monogem Pulsar TeV halo**SUNIL MALIK,<sup>1,2</sup> KA HO YUEN,<sup>3</sup> AND HUIRONG YAN<sup>1,2</sup><sup>1</sup>*Institute für Physik und Astronomie Universität Potsdam, Golm Haus 28, D-14476 Potsdam, Germany*<sup>2</sup>*Deutsches Elektronen-Synchrotron DESY, Platanenallee 6, 15738 Zeuthen, Germany*<sup>3</sup>*Theoretical Division, Los Alamos National Laboratory, Los Alamos, NM 87545, USA***ABSTRACT**

Magnetic fields are ubiquitous in the interstellar medium, including extended objects such as supernova remnants (SNRs) and Pulsar Wind Nebulae (PWNe). Its turbulent characteristics govern the diffusion of cosmic rays and the multi-wavelength emission from PWNe. However, the geometry and turbulence nature of the magnetic fields in the ambient region of PWN is still unknown. Recent gamma-ray observations from HAWC and synchrotron observations suggest a highly suppressed diffusion coefficient compared to the mean interstellar value. In this letter, we present the first direct observational evidence that the local mean magnetic field is nearly aligned toward the line of sight (LoS) with an inclination angle  $\theta_\lambda < 10^\circ$  employing a recently developed statistical recipe known as ‘Y-parameter’. Furthermore, we report that the magnetic field fluctuations are mostly dominated by compressible modes, with a 2D correlation length of approximately 3 pc in the vicinity of Monogem PWN region. Our study highlights the pivotal role of magnetic field and turbulence in unraveling the physical processes in TeV halos and cosmic ray transport.

**Keywords:** Magnetic field – polarization, Stokes parameters, objects: Pulsar wind nebulae, general – interstellar medium, Turbulence – techniques: synchrotron radiation, Cosmic Ray emission, Star formation, Particle Transport

**1. INTRODUCTION**

The interstellar medium (ISM) and extended objects such as pulsar wind nebulae (PWNe) and supernova remnants (SNRs) are permeated by the magnetic fields. This magnetic field exhibits a complex structure, spanning a wide range of strengths from  $\mu\text{G}$  to  $\text{mG}$  (Reynolds et al. 2012). The turbulent characteristics of this magnetic field play a crucial role in facilitating various physical processes, including particle transport and acceleration (Schlickeiser 2002; Yan & Lazarian 2002; Yan et al. 2012; Lemoine 2022; Yan 2022). Magnetohydrodynamic (MHD) turbulence is classified into the incompressible Alfvénic mode and the compressible modes (Cho & Lazarian 2003; Lazarian & Pogosyan 2012; Makwana & Yan 2020), and it interacts significantly with cosmic rays, governing their scattering and diffusion across different phases of the ISM as well as in the ambient regions of extended objects (Yan & Lazarian 2004, 2008). Therefore, to comprehensively understand cosmic ray diffusion and multi-wavelength emissions in the vicinity of PWNe, it

is essential to investigate the underlying magnetic field configuration and the nature of the associated turbulence.

Recent studies (Liu et al. 2019b; Breuhaus et al. 2022; Mukhopadhyay & Linden 2022) have investigated the TeV’s halo observations from PWNe using a theoretical spectrum generated through a combination of synchrotron radiation and inverse-Compton (IC) scattering from the same population of energetic electrons. The authors suggest that the suppressed diffusion in the ambient region of PWNe can be attributed to the topology of the local magnetic fields.

However, the direct observation of the orientation and strength of the magnetic field in the ambient halo region of pulsars has proven to be challenging. To address this issue, our recent study has employed turbulence mapping theory based on synchrotron emission statistics, presenting a novel statistical approach using the Y-parameter (Malik et al. 2023). This technique has the potential to unveil the 3D geometry of magnetic fields and their dominant MHD turbulence characteristics. In this paper, we utilize the Y-parameter technique to provide the first observational investigation to constrain the magnetic field direction within these halos.

This paper is structured as follows: In Section 2, we examine the characteristics of the PWN TeV halo, with particular emphasis on the Monogem halo. Our primary analysis of

sunil.malik@uni-potsdam.de

kyuen@lanl.gov

huirong.yan@desy.de (Corresponding author)

diagnosing the local magnetic field inclination angle, utilizing the recently developed turbulence anisotropy analysis and the multi-points structure function, is described in Section 3. The discussions and summary of our findings are presented in Section 4 and 5, respectively.

## 2. CHARACTERISTIC OF PWN TEV HALO

The HAWC collaboration recently made notable discoveries of potential TeV sources, namely 2HWC J0635+180 and 2HWC J0700+143 (Abeysekara et al. 2017a), in the nearby PWN Geminga and PSR B0656+14 (Monogem) at significance levels of  $13.1\sigma$  and  $8.1\sigma$  respectively (Abeysekara et al. 2017a,b). These sources are located at a relatively short distance from Earth, with Geminga at 250 pc and Monogem at 288 pc. The diffusive propagation of particles within these halos extends to approximately 10 – 50 pc, which points to a much slower diffusion coefficient compared to the Galactic mean, presenting a challenge in comprehending the underlying mechanisms responsible for the observed high-energy emissions (Abeysekara et al. 2017b).

In Liu et al. (2019b), the authors proposed a promising model for explaining the TeV observations of the Geminga PWN using anisotropic diffusion. In the case of sub-Alfvénic turbulence, the diffusion coefficients perpendicular and parallel to the mean magnetic field show significant differences (i.e.,  $D_{\perp} \sim D_{\parallel} M_A^4$ ) (where  $D_{\perp}$ ,  $D_{\parallel}$  is diffusion coefficient in perpendicular and parallel direction of the magnetic field, respectively,  $M_A$  represents Alfvénic Mach Number) (Yan & Lazarian 2008; Giacinti & Sigl 2012; López-Coto & Giacinti 2018; Maiti et al. 2022). The authors of this theoretical model inferred that local magnetic fields with small inclination angles relative to the line of sight could account for the observed TeV emissions and the phenomenon of suppressed diffusion. Currently, direct measurements of the magnetic field strength and orientation are not feasible due to the absence of synchrotron polarized emissions in the vicinity of the Geminga PWN.

To get the first direct observational evidence, in this study, we focus on Monogem PWN (PSR B0656+14) which is observed in multi-wavelength from radio to gamma rays (Uyaniker et al. 1999; Johnston et al. 2006, 2007; Abeysekara et al. 2017b). It has a period (P) of approximately 385 ms, period derivative ( $\dot{P} \sim 5.4 \times 10^{-14} \text{ s s}^{-1}$ ) corresponding<sup>1</sup> to a spin-down age ( $\tau$ ) of approximately 111 kyr, a spin-down power ( $E_{\text{rot}}$ ) of  $3.8 \times 10^{34} \text{ erg s}^{-1}$ , and a surface magnetic field ( $B_{\text{surf}}$ ) of approximately  $4.65 \times 10^{12} \text{ G}$ .

## 3. 3D MAGNETIC FIELD FROM TURBULENCE ANALYSIS

### 3.1. Synchrotron Polarisation Observations

In order to investigate the strength and morphology of magnetic fields in the Monogem PWN TeV halo region, we

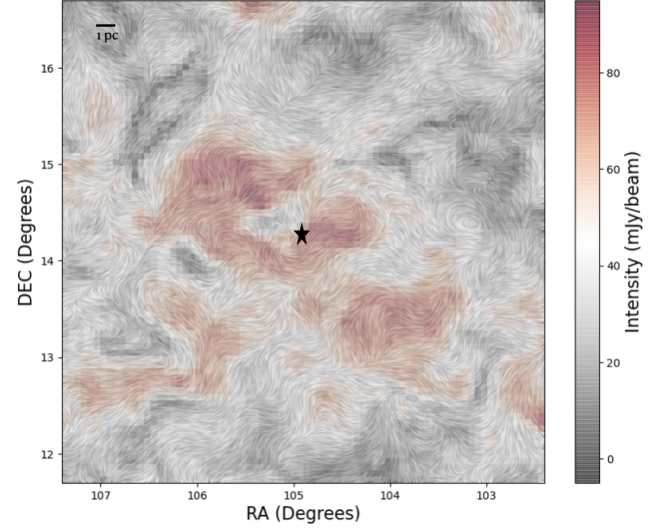


**Figure 1.** The synchrotron polarisation emission map of Monogem (B0656+14) PWN ( $5^\circ \times 5^\circ$ ) with the center indicated by star symbol at R.A.(J2000) =  $06^{\text{h}}59^{\text{m}}48^{\text{s}}.02$  ( $104.94^\circ$ ), Dec.(J2000) =  $14^\circ14'19''.4$  ( $14.23^\circ$ ) using Effelsberg 100-m telescope observation at 1.4 GHz from Uyaniker et al. (1999). Here the color bar represents the flux in mJy/beam. The streamline, computed via the Line Integral Convolution (LIC) algorithm (Cabral & Leedom 1993, Zöckler et al. 1997), represents the direction of the magnetic field inferred from the synchrotron polarisation observations.

utilized the Effelsberg 100-m 21 cm POL<sup>2</sup> survey. This survey, conducted at medium Galactic latitudes, involves radio continuum and polarization observations. The data were obtained using the Effelsberg 100-m telescope at a frequency of 1.4 GHz, with an angular resolution of  $9.35'$  (Uyaniker et al. 1999).

We specifically employed  $5^\circ \times 5^\circ$  synchrotron polarization observations of the Monogem (B0656+14) pulsar region, as depicted in Fig. 1. The observation map was overlaid with streamlines computed using the Line Integral Convolution (LIC) algorithm, which indicates the inferred direction of the magnetic field based on the polarization direction (Cabral & Leedom 1993; Zöckler et al. 1997). The figure exhibits a significant increase in linearly polarized flux in and around the vicinity of the Monogem Pulsar, which is indicated by the black star symbol. The observed variations in streamlining suggest a 2D Alfvén Mach number in the pictorial plane approximately  $M_{A,2D} \approx 1.0$ . Utilizing this map, we examined the magnetic field topology in the surrounding region of the Monogem PWN.

### 3.2. Correlation length from Structure-Function Analysis

In polarisation observations, the large-scale magnetic fields can coexist with the small-scale turbulent components.

<sup>1</sup> See e.g. Lorimer & Kramer (2004) for the formulae used to derive  $\tau$ ,  $\dot{E}_{\text{rot}}$  and  $B_{\text{surf}}$  using P and  $\dot{P}$

<sup>2</sup> <https://www3.mpifr-bonn.mpg.de/survey.html>

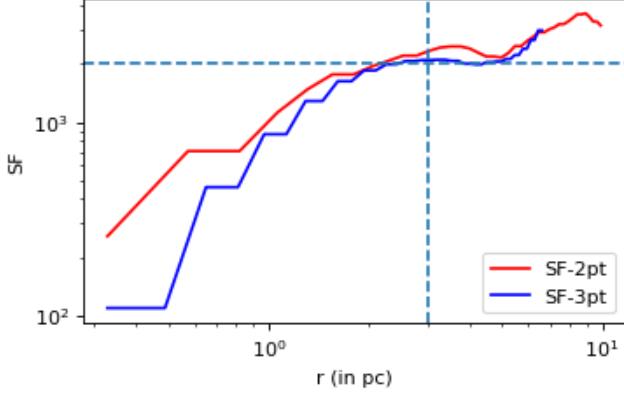


**Figure 2.** The multi-point structure function for the total polarised intensity. Different colors correspond to different points' structure functions. The vertical and horizontal lines indicate the plateau stage. These different structure functions are estimated by using Eq. 1 & 2.

In recent studies (Hildebrand et al. 2009; Pattle et al. 2017; Cho 2019) several approaches have been discussed to address this issue, including the fitting method and wavelet transformation (Grebenev et al. 1995). These techniques heavily rely on data coarsening. One widely accepted and commonly used method for assessing fluctuations is through two-point structure function (SF), defined as follows:

$$SF_2^{2pt}(\mathbf{R}) = \langle |X(\mathbf{R}' + \mathbf{R}) - X(\mathbf{R})|^2 \rangle_{\mathbf{R}'} \quad (1)$$

where  $X$  represents an observable in the plane of the sky.  $SF_2^{2pt}$  will be an increasing function of  $\mathbf{R}$  when we are in the regime of  $\mathbf{R} < L_s$ , here  $L_s$  represents the correlation length of small-scale fluctuations. It will attain a plateau for  $\mathbf{R} \gtrsim L_s$ . However, the shape of  $SF_2^{2pt}$  gets distorted in the presence of large-scale gradients in the observables. In this case, three and more point structure functions can be utilized to remove these large-scale variations (Cho 2019). The three points SF is expressed as;

$$SF_2^{3pt}(\mathbf{R}) = \frac{1}{3} \langle |X(\mathbf{R}' - \mathbf{R}) - 2X(\mathbf{R}') + X(\mathbf{R}' + \mathbf{R})|^2 \rangle_{\mathbf{R}'} \quad (2)$$

The two-point structure function is represented by the red line in Fig 2. From the plot, it is evident that our region near Monogem PWN exhibits both large-scale gradients and small-scale fluctuations in the magnetic field. The three points (3 pts) SF is depicted by the blue line in Fig.2. We want to emphasize that evaluating structure functions with more than two points limits us to smaller length scales, as evident in our SF plot in Fig.2.

Consequently, we determined that the region possesses a characteristic correlation length of approximately 3 pc for the local MHD turbulence, based on the synchrotron map. Furthermore, we can employ this 2D correlation length,  $R \sim 3$  pc, to conduct a turbulence anisotropy analysis known as the 'Y-parameter' (Malik et al. 2023).

### 3.3. Line of sight inclination angle of B-field from Y-parameter Analysis

To measure the relative angle between the mean magnetic field and the line of sight, we employ a recently developed technique called the "y-parameter analysis" (Malik et al. 2023). It was suggested in earlier literature that the anisotropy of the Stokes parameters can be used to infer the geometric properties of the magnetic field. The global correlation function, represented as  $D_X$ , can effectively capture the anisotropy of a given observable, denoted as  $X$ , which can be expressed as follows:

$$D_X(\mathbf{R}) = \langle (X(\mathbf{R}')X(\mathbf{R}' + \mathbf{R}))^2 \rangle_{\mathbf{R}'}. \quad (3)$$

Malik et al. (2023) suggest that the 'Y-parameter', which is expressed as:

$$Y = \frac{\text{Anisotropy}(D_{I+Q})}{\text{Anisotropy}(D_{I-Q})} = \frac{v/h(D_{I+Q})}{v/h(D_{I-Q})}. \quad (4)$$

can be used to trace the inclination angle of the magnetic field. Here,  $v$  and  $h$  represent the vertical and horizontal dimensions relative to  $B_\perp$ . This statistical parameter, derived from polarized synchrotron radiation, captures the variations in the embedded magnetic fields resulting from turbulence. Consequently, it enables us to investigate the geometry of the 3D magnetic field and the characteristics of the underlying MHD turbulence. We established a statistical criterion of  $Y \sim 1.5 \pm 0.5$  (with  $Y > 1.5$  indicating the A mode and  $Y < 1.5$  indicating the C mode) to identify the dominant fraction of MHD turbulence modes. Remarkably, the Y-parameter for different modes exhibited contrasting trends (either decreasing or increasing) with respect to the local mean magnetic field inclination angle, denoted as  $\theta_\lambda$ .

To estimate the mean-field inclination angle for the vicinity of the Monogem TeV halo, we applied the technique described earlier to synchrotron polarization observations (Fig.1) within a ( $5^\circ \times 5^\circ$ ) region around the Monogem pulsar. We initially analyzed the correlation function of  $I + Q \propto B_x^2$  and  $I - Q \propto B_y^2$  and plotted the results in Fig. 3. These correlation function plots clearly depict the difference in horizontal and vertical lengths relative to the mean magnetic field direction. To quantify the anisotropies, we performed 2D Gaussian fittings on these distributions by keeping the fitting radius within the 2D correlation length of 3.0 pc and obtained  $Y \approx 0.83$ . According to our previous investigation in Malik et al. (2023), a  $Y < 1.0$  implies a mean magnetic field inclination angle of  $\theta_\lambda < 10^\circ$  and indicates that the local turbulence is predominantly of compressible nature.

These results clearly indicate that the vicinity of the PWN exhibits a mean magnetic field that is potentially aligned with the line of sight, along with the presence of compressible turbulence. This alignment is crucial for the propagation of cosmic rays (Yan & Lazarian 2008). Importantly, our analysis provides direct observational confirmation for the speculation that the magnetic fields in such TeV halos are not in the extreme limit, as suggested in the existing literature. This finding offers reassurance regarding the effectiveness of the

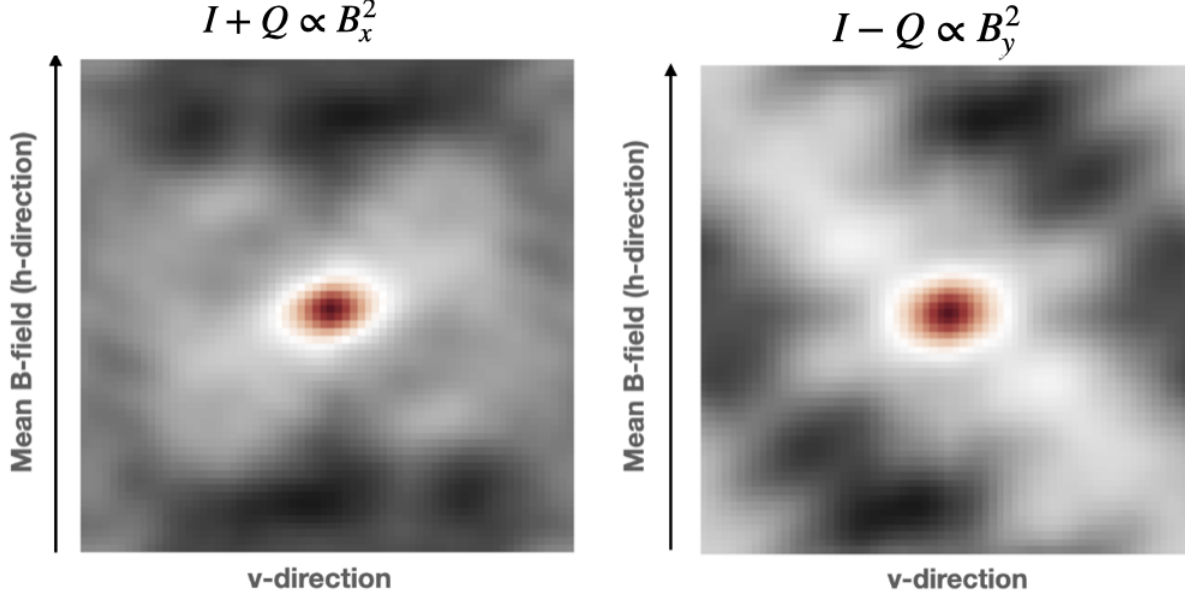


**Figure 3.** *Left panel:* This figure shows the correlation function distribution for the  $I + Q \propto B_x^2$ . *Right panel:* It is same as the left but for  $I - Q \propto B_y^2$ . Here we have drawn a vertical arrow to indicate the direction of the mean B-field in the  $5^\circ \times 5^\circ$  region of interest around the Monogem pulsar.

Y-parameter technique in retrieving 3D magnetic fields in various environments, including the ISM and extended objects such as PWNe and SNRs.

#### 4. DISCUSSION

As discussed in Section 1, MHD turbulence plays a crucial role in the acceleration and scattering of cosmic rays in the ISM and other extended objects. The recent discovery of TeV halos around middle-aged pulsars, such as Geminga and Monogem (PSR B0656+14), has raised intriguing questions, particularly the origin of the slower diffusion (Abeysekara et al. 2017b). In a recent study by Liu et al. (2019b), it was proposed that sub-Alfvénic turbulence combined with a local mean magnetic field aligned with the line of sight can account for the missing X-ray flux as well as the slow diffusion since  $D_\perp = D_\parallel M_A^4$ . Therefore, to obtain a comprehensive understanding of these observations, it is crucial to directly investigate the 3D magnetic field strength, orientation, and the underlying MHD turbulence.

To investigate the magnetic field topology in extended objects such as TeV halos associated with PWNe and supernova remnants, direct observational evidence is currently lacking. A recent study by Liu et al. (2019a) has suggested an upper limit of  $0.8 \mu\text{G}$  for the magnetic field in the Geminga PWN, which is lower than the average galactic magnetic field strength ( $\sim 5.5 \mu\text{G}$ , Sofue et al. 2019). The absence of radio-polarized emission in the vicinity of Geminga has hindered direct observations of the magnetic field strength and associated turbulence in that region.

In this study, we employ radio synchrotron polarization statistics from a  $(5^\circ \times 5^\circ)$  region around the Monogem PWN to infer the nature of the 3D magnetic field and its turbulence

using our Y-parameter technique, as described in Malik et al. (2023). Our analysis yielded a value of  $Y \sim 0.83$  based on the 2D coherence length scale estimated using the structure-function in Fig. 2. Following the criteria established in Malik et al. (2023), we have identified two potential scenarios: one with  $\theta_\lambda \lesssim 10^\circ$  dominated by compressible modes, and the other with  $\theta_\lambda > 60^\circ$  characterized by Alfvénic turbulence. Analysis of simulated MHD datacubes favours the first scenario over the others.

Furthermore, in the Monogem TeV halo, the required diffusion coefficient is also significantly suppressed compared to the ISM value, similar to the case of the Geminga TeV halo. This suppressed diffusion, combined with the small  $\theta_\lambda$  angle, suggests that cross-field transport with  $D_\perp \propto D_\parallel M_A^4$  serves as the underlying mechanism for the reduced diffusion (Yan & Lazarian 2008). Assuming  $D_\parallel \simeq D_{ISM} \sim 3.8 \times 10^{28}$ , the average ISM diffusion coefficient as adopted in Liu et al. (2019b), we estimate a local Alfvénic Mach number  $M_A \sim 0.2$ . The results obtained using various diagnostics are summarized in the table below.

Diagnostics	Measure	Values
Y-parameter	$\theta_\lambda$	$< 10^\circ$
Structure Function	$L_{coh, 2D}$	$\sim 3.0 \text{ pc}$
Polarisation Angle	$M_{A, 2D}$	1.0
$D_\perp / D_\parallel$	$M_{A, 3D}$	$\gtrsim 0.2$

**Table 1.** We have listed all the estimated quantities in this study.



Additionally, in the halo-like environment, there are limited methods to gain insight into the strength of the parallel magnetic field component ( $B_{\parallel}$ ). The rotation and dispersion measures of the pulsar might offer some clues about the  $B_{\parallel}$ <sup>3</sup> component of the magnetic field, but are also affected by foreground contamination. In any case, the magnetic field orientation can not be inferred from the observations of pulsars themselves. Therefore, our study facilitates a pivotal advancement in the understanding of magnetism and the underlying physical process governing the TeV-PeV halos associated with PWN and SNRs.

## 5. CONCLUSIONS

In this letter, we have presented the first observation analysis of magnetic field 3D geometry and underlying MHD turbulence nature in the TeV halo associated with the Monogem PWN using various probes from multi-wavelength observations. Our structure-function analysis shows that the region has a pictorial plane correlation length of  $\sim 3$  pc for the lo-

cal MHD turbulence. Further, the Y-parameter analysis using synchrotron polarisation observations with  $Y \sim 0.83$  suggests that the local mean magnetic field has an inclination angle  $\theta_{\lambda} < 10^{\circ}$  and is dominated by compressible turbulence fluctuations, both of which contribute to the suppressed diffusion of cosmic rays as observed by HAWC (Abeysekara et al. 2017b).

Thus our study underpins the crucial role of the magnetic field in understanding the physical processes involved in recent and future detections of such extraordinary high-energy emissions in the Milky Way.

## ACKNOWLEDGMENTS

SM would like to thank Parth Pavaskar, Siqi Zhao, and Bingqiang Qiao for the helpful discussions. The research presented in this article was partially supported by the Laboratory Directed Research and Development program of Los Alamos National Laboratory under project number(s) 20220700PRD1.

## REFERENCES

- Abeysekara, A. U., Albert, A., Alfaro, R., et al. 2017a, *ApJ*, 843, 39, doi: [10.3847/1538-4357/aa7555](https://doi.org/10.3847/1538-4357/aa7555)
- . 2017b, *Science*, 358, 911, doi: [10.1126/science.aan4880](https://doi.org/10.1126/science.aan4880)
- Breuhaus, M., Reville, B., & Hinton, J. A. 2022, *A&A*, 660, A8, doi: [10.1051/0004-6361/202142097](https://doi.org/10.1051/0004-6361/202142097)
- Cabral, B., & Leedom, L. C. 1993, in *Proceedings of the 20th Annual Conference on Computer Graphics and Interactive Techniques, SIGGRAPH '93* (New York, NY, USA: Association for Computing Machinery), 263–270, doi: [10.1145/166117.166151](https://doi.org/10.1145/166117.166151)
- Cho, J. 2019, *ApJ*, 874, 75, doi: [10.3847/1538-4357/ab06f3](https://doi.org/10.3847/1538-4357/ab06f3)
- Cho, J., & Lazarian, A. 2003, *MNRAS*, 345, 325, doi: [10.1046/j.1365-8711.2003.06941.x](https://doi.org/10.1046/j.1365-8711.2003.06941.x)
- Giacinti, G., & Sigl, G. 2012, *Phys. Rev. Lett.*, 109, 071101, doi: [10.1103/PhysRevLett.109.071101](https://doi.org/10.1103/PhysRevLett.109.071101)
- Grebenev, S. A., Forman, W., Jones, C., & Murray, S. 1995, *ApJ*, 445, 607, doi: [10.1086/175725](https://doi.org/10.1086/175725)
- Hildebrand, R. H., Kirby, L., Dotson, J. L., Houde, M., & Vaillancourt, J. E. 2009, *ApJ*, 696, 567, doi: [10.1088/0004-637X/696/1/567](https://doi.org/10.1088/0004-637X/696/1/567)
- Johnston, S., Karastergiou, A., & Willett, K. 2006, *MNRAS*, 369, 1916, doi: [10.1111/j.1365-2966.2006.10440.x](https://doi.org/10.1111/j.1365-2966.2006.10440.x)
- Johnston, S., Kramer, M., Karastergiou, A., et al. 2007, *MNRAS*, 381, 1625, doi: [10.1111/j.1365-2966.2007.12352.x](https://doi.org/10.1111/j.1365-2966.2007.12352.x)
- Lazarian, A., & Pogosyan, D. 2012, *ApJ*, 747, 5, doi: [10.1088/0004-637X/747/1/5](https://doi.org/10.1088/0004-637X/747/1/5)
- Lemoine, M. 2022, *Phys. Rev. Lett.*, 129, 215101, doi: [10.1103/PhysRevLett.129.215101](https://doi.org/10.1103/PhysRevLett.129.215101)
- Liu, R.-Y., Ge, C., Sun, X.-N., & Wang, X.-Y. 2019a, *ApJ*, 875, 149, doi: [10.3847/1538-4357/ab125c](https://doi.org/10.3847/1538-4357/ab125c)
- Liu, R.-Y., Yan, H., & Zhang, H. 2019b, *Phys. Rev. Lett.*, 123, 221103, doi: [10.1103/PhysRevLett.123.221103](https://doi.org/10.1103/PhysRevLett.123.221103)
- López-Coto, R., & Giacinti, G. 2018, *MNRAS*, 479, 4526, doi: [10.1093/mnras/sty1821](https://doi.org/10.1093/mnras/sty1821)
- Lorimer, D. R., & Kramer, M. 2004, *Handbook of Pulsar Astronomy*, Vol. 4
- Maiti, S., Makwana, K., Zhang, H., & Yan, H. 2022, *ApJ*, 926, 94, doi: [10.3847/1538-4357/ac46c8](https://doi.org/10.3847/1538-4357/ac46c8)
- Makwana, K. D., & Yan, H. 2020, *Physical Review X*, 10, 031021, doi: [10.1103/PhysRevX.10.031021](https://doi.org/10.1103/PhysRevX.10.031021)
- Malik, S., Yuen, K. H., & Yan, H. 2023, *MNRAS*, accepted for publication, arXiv:2303.17282. <https://arxiv.org/abs/2303.17282>
- Mukhopadhyay, P., & Linden, T. 2022, *Phys. Rev. D*, 105, 123008, doi: [10.1103/PhysRevD.105.123008](https://doi.org/10.1103/PhysRevD.105.123008)
- Pattle, K., Ward-Thompson, D., Berry, D., et al. 2017, *ApJ*, 846, 122, doi: [10.3847/1538-4357/aa80e5](https://doi.org/10.3847/1538-4357/aa80e5)
- Reynolds, S. P., Gaensler, B. M., & Bocchino, F. 2012, *SSRv*, 166, 231, doi: [10.1007/s11214-011-9775-y](https://doi.org/10.1007/s11214-011-9775-y)
- Schlickeiser, R. 2002, *Cosmic Ray Astrophysics*, 183
- Sofue, Y., Nakanishi, H., & Ichiki, K. 2019, *MNRAS*, 485, 924, doi: [10.1093/mnras/stz407](https://doi.org/10.1093/mnras/stz407)
- Uyaniker, B., Fürst, E., Reich, W., Reich, P., & Wielebinski, R. 1999, *A&AS*, 138, 31, doi: [10.1051/aas:1999494](https://doi.org/10.1051/aas:1999494)
- Yan, H. 2022, in *37th International Cosmic Ray Conference*, 38, doi: [10.22323/1.395.0038](https://doi.org/10.22323/1.395.0038)

<sup>3</sup> Using RM of  $22.73 \pm 8.0$  rad m<sup>-2</sup> and DM of  $13.7 \pm 0.2$  pc cm<sup>-3</sup>, we can estimate the  $B_{\parallel} \sim 2.04 \pm 0.72 \mu\text{G}$ .

- Yan, H., & Lazarian, A. 2002, *Phys. Rev. Lett.*, 89, 281102, doi: [10.1103/PhysRevLett.89.281102](https://doi.org/10.1103/PhysRevLett.89.281102)
- . 2004, *ApJ*, 614, 757, doi: [10.1086/423733](https://doi.org/10.1086/423733)
- . 2008, *ApJ*, 673, 942, doi: [10.1086/524771](https://doi.org/10.1086/524771)
- Yan, H., Lazarian, A., & Schlickeiser, R. 2012, *ApJ*, 745, 140, doi: [10.1088/0004-637X/745/2/140](https://doi.org/10.1088/0004-637X/745/2/140)
- Zöckler, M., Stalling, D., & Hege, H.-C. 1997, *Parallel Computing*, 23, 975, doi: [https://doi.org/10.1016/S0167-8191\(97\)00039-2](https://doi.org/10.1016/S0167-8191(97)00039-2)